

# Steroid Cell Tumours: Rare Ovarian Tumours that Cause Hyperandrogenaemia in Postmenopausal Women

xiaodan zhu

First Hospital of Zhejiang Province: Zhejiang University School of Medicine First Affiliated Hospital

liny zhou

First Hospital of Zhejiang Province: Zhejiang University School of Medicine First Affiliated Hospital

jian jiang

First Hospital of Zhejiang Province: Zhejiang University School of Medicine First Affiliated Hospital

Tian'an Jiang (✉ [tiananjiang@zju.edu.cn](mailto:tiananjiang@zju.edu.cn))

the first affiliated hospital, college of medicine, Zhejiang University <https://orcid.org/0000-0002-7672-8394>

---

## Case report

**Keywords:** hyperandrogenaemia, tumours, postmenopausal

**Posted Date:** December 29th, 2020

**DOI:** <https://doi.org/10.21203/rs.3.rs-136187/v1>

**License:**  This work is licensed under a Creative Commons Attribution 4.0 International License.

[Read Full License](#)

---

# Abstract

**Background** Diagnosing hyperandrogenemia in postmenopausal women is very difficult, because it occasionally manifests as excessive hair growth or no clinical manifestations, so it is often misdiagnosed or missed diagnosis. Ovarian steroid cell tumours that cause hyperandrogenaemia in women account for approximately 0.1% of all ovarian tumours. Due to the low incidence, corresponding imaging reports are rare, so ovarian steroid cell tumours lacks typical imaging findings to differentiate it from other ovarian tumours. Therefore, we summarized its clinical and imaging characteristics through this case series, and we also elaborated on the differential diagnosis of steroid cell tumors. We hope to help clinicians have a deeper understanding of ovarian steroid cell tumours.

**Case presentation** we report three cases of postmenopausal women with hyperandrogenaemia. Only 1 patient showed virilization symptoms, the other two patients were completely asymptomatic. All patients underwent total hysterectomy + bilateral adnexectomy. Histological results showed one case of leydig cell tumor (case 1) and two cases of benign non-specific steroid cell tumor (case 2 and case 3). After the operation, the androgen levels of all patients returned to normal, and there was no clinical recurrence since follow-up.

**Conclusions** Through this series of cases, we found that although virilization caused by increased serum testosterone levels is an important clinical feature of ovarian steroid cell tumors, complete asymptomatic is also one of its features. A solid, slightly hypoechoic, round or oval mass with uniform internal echo, richer blood flow in the solid part and low resistance index are typical imaging features of ovarian steroid cell tumors. Diagnosis of ovarian steroid cell tumours after menopause is challenging, but surgery can be used for both diagnosis and clear treatment.

## Background

Female androgenaemia can cause virilization syndromes, such as progressive hirsutism, acne, vocal cord thickening, amenorrhea, breast atrophy, and male pattern baldness. However, the diagnosis of postmenopausal women with hyperandrogenaemia is very difficult because the clinical manifestations are commonly absent or comprise mostly hair overgrowth, so the disease is often attributed to normal hormonal changes with ageing. Diseases that cause hyperandrogenaemia in women include ovarian functional tumours, polycystic ovary syndrome, congenital adrenal hyperplasia, congenital follicular cell hyperplasia, acanthosis nigricans, and Cushing's syndrome, among others <sup>[1]</sup>. Ovarian steroid cell tumours (OSCTs) are a type of functional tumour and account for approximately 0.1% of all ovarian tumours <sup>[2]</sup>. In 2014, the WHO divided them into ovarian steroid cell tumour, not otherwise specified (OSCT-NOS) lesions and ovarian Leydig cell tumours (OLCTs) <sup>[3]</sup>. OLCTs are very rare, mainly benign, and more common in menopausal women. These tumours usually occur on one side of the ovary and are small and solid <sup>[4]</sup>. Most OSCT-NOS lesions consist of a solid, oval mass with a regular shape that occurs on one side of the ovary. The average age of onset is 42 years. Occurrences in postmenopausal women or children are rare <sup>[5, 6]</sup>.

# Case Presentation

## Case 1

A 60-year-old female who had been menopausal for 7 years presented with a progressive increase in body hair lasting for 6 months. She had a history of uterine fibroids and diabetes and was currently taking "metformin tablets, 0.5 g (Bid), and glimepiride tablets, 2 mg (Qd)". Laboratory examination revealed the following (Table 1): the serum testosterone hormone level was significantly increased (504.5 ng/dl), and the levels of other sex hormones and tumour markers were normal. A mid-dose dexamethasone suppression test showed that testosterone was not suppressed (before inhibition: androstenedione, 3.7 ng/ml; testosterone, 504.5 ng/dl; and dehydroepiandrosterone sulphate, 65.5 µg/dl; after inhibition: androstenedione, 1.6 ng/ml; testosterone, 244.7 ng/dl; dehydrosulphate epiandrosterone, 42.1 µg/dl; and 17a hydroxyprogesterone, 0.1 nmol/L). Physical examination revealed an increased amount of relatively long facial hair, pubic hair and body hair in the groin area. No skin pigmentation, voice thickening, weight gain, facial fattening, abdominal circumference thickening or other symptoms were observed. Imaging examinations were performed (Table 2). Transvaginal ultrasonography (TVS) revealed atrophy of the uterus and bilateral ovaries. A slightly hyperechoic nodule with a diameter of approximately 1.23 cm was observed in the right ovary, with an unclear boundary (Fig. 1A). Unfortunately, no blood flow images were available. Enhanced magnetic resonance imaging (MRI) of the pelvis (Fig. 3A) showed nodules in the right adnexal area, suggesting ovarian cysts. Contrast-enhanced computed tomography (CT) of the pelvis (Fig. 3B) showed high-density shadows in the nodular tip of the right adnexal area, suggesting a sex cord-stromal tumour. The patient underwent total hysterectomy + bilateral adnexectomy. A grey-white nodule with a diameter of approximately 1.7 cm was observed on the cut surface of the pathological specimen after the operation. Pathology indicated an LCT (Fig. 4A): calretinin (CR) (+), chromogranin A (CgA) (-), cytokeratin (CK) (pan) (focus +), inhibin A (+), Ki-67 (6%), S-100 (-), CD99 (-), and smooth muscle actin (SMA) (-). The testosterone level of the patient was 57.1 ng/dl on the first postoperative day; the virilization symptoms gradually subsided, and there were no signs of clinical recurrence.

Table 1  
Biochemical parameters determined before and after surgery

Result	Patient 1		Patient 2		Patient 3	
	Before surgery	After surgery	Before surgery	After surgery	Before surgery	After surgery
LH (mUI/mL)(11.3–40.0)	9.91	18.58	16.98	38.61	6.72	ND
FSH (mUI/mL)(9.7–111.0)	22.9	48.7	20.75	107.99	14.88	ND
Total testosterone (ng/dL) (10.83–56.94)	504.5	35.7	258.09	17.5	326.03	21.25
Oestradiol (pg/mL) (< 30)	51	11.8	73.21	10	71.38	ND
Progesterone(ng/mL)	0.49	0.3	0.43	0.1	0.24	ND
Androstenedione (ng/mL) (0.3–3.3)	1.6	ND	2	ND	1.7	ND
DHEAS (mg/dL)	42.1	ND	50.5	ND	44.3	ND
17 OHP (ng/mL) (0.2–1.7)	1.7	ND	ND	ND	ND	ND
17 OHP (ng/mL) 600 after ACTH stimulation test	0.1	ND	ND	ND	ND	ND
17 OHP, 17 hydroxyprogesterone; ACTH, Adrenocorticotrophic hormone; DHEA-S, dehydroepiandrosterone-sulfate; FSH, follicle-stimulating hormone; LH, luteinizing hormone; ND, not done.						

Table 2  
Radiological features

	Patient 1	Patient 2	Patient 3
Pelvic ultrasound	Hyperechoic nodule of Ro(12.3 mm)	Hyperechoic mass of Lo(34*22 mm)	Hyperechoic mass of Lo(45*20 mm)
Pelvic CT	Nodular slightly dense shadow of Ro with visible enhancement after enhancement	ND	Oval slightly lower density mass of left adnexal area uneven enhancement after enhancement, continuous enhancement in venous phase
Pelvic MRI	Round-shaped abnormal signal range of Ro, T2W1 and DW1 are high signal, higher signal area can be seen in the center	A circular signal shadow of Lo, equal to T1 long and T2 signal, DWI high signal, and obviously enhanced after enhancement	ND
Ro, right ovary; Lo, left ovary; ND, not done.			

## Case 2

A 55-year-old female who had been menopausal for 5 years presented with a mass in the left appendix area lasting for 5 months on physical examination; the mass had recently significantly increased in size. The patient was in good health and had no history of special chronic diseases. Laboratory examination revealed the following (Table 1): the serum testosterone hormone level was significantly increased (258.09 ng/dl), and the levels of other sex hormones and tumour markers were normal. There were no obvious abnormalities on physical examination. Imaging examinations were performed (Table 2). TVS revealed atrophy of the uterus. The left ovary showed a slightly hyperechoic mass of approximately 3.0\*2.2\*3.4 cm in size (Fig. 1B), with clear borders. Colour Doppler flow imaging (CDFI) showed an abundant blood supply (Fig. 2A), with a resistance index (RI) of 0.39. Enhanced MRI of the pelvis revealed a space-occupying mass in the left adnexal area, suggesting a sex cord-stromal tumour (Fig. 3C). The patient underwent total hysterectomy + bilateral adnexectomy. A clear, greyish-yellow, round nodule was observed on pathology after surgery, with a diameter of 2.3\*3.0 cm. Pathology showed an SCT-NOS lesion (Fig. 4B): CK7 (-), CK (pan) (-), paired-box gene 8 (PAX-8) (-), inhibin A (+), CR (+), placental alkaline phosphatase (PLAP) (-), Wilms' tumour gene (WT1) (-), Oct-4 (-), glypican 3 (GPC-3) (-), beta human chorionic gonadotropin ( $\beta$ -HCG) (-), Ki-67 (+, 3%), CD99 (+), S-100 (-), CD117 (-), CD30 (weak +), net dye (+), and E-cadherin (-). The testosterone level of the patient was 17.5 ng/dl after the operation, and the postoperative course was uneventful.

## Case 3

A 52-year-old female who had been menopausal for 1 year presented with ovarian cysts found on physical examination 1 month prior. The patient had a past history of hypertension, adenomyosis with

multiple uterine fibroids, and bilateral kidney cysts. Laboratory examination (Table 1): the serum testosterone hormone level was significantly increased (326.03 ng/dl), and the levels of other sex hormones and tumour markers were normal. There were no obvious abnormalities on physical examination. Imaging examinations were performed (Table 2). TVS indicated a trend of uterine atrophy, with cystic and solid changes in the left ovary. A solid, slightly hyperechoic mass of approximately 4.3\*2.9\*2.8 cm in size was observed in the left ovary (Fig. 1C), with clear boundaries. CDFI showed an abundant blood supply in the mass (Fig. 2B), with an RI of 0.55. Enhanced CT of the pelvis showed a solid/cystic mass in the left adnexal area, suggesting a left uterine broad ligament fibroid with central degeneration (Fig. 3D). The patient underwent total hysterectomy + bilateral appendectomy. Intraoperative dissection showed that the left ovarian fluid was yellow and turbid, the cyst wall was thickened, and the inner section consisted of tough, yellowish tissue. Pathology indicated an SCT-NOS lesion: CK (pan) (part +), oestrogen receptor (ER) (-), progesterone receptor (PR) (-), inhibin A (+), CR (+), WT1 (-), human melanoma black 45 (HMB-45) (-), MelanA (+), CgA (-), synaptophysin (Syn) (-), Desmin (-), Ki-67 (+, 20%), CD34 (-), and epithelial membrane antigen (EMA) (-). The testosterone level of the patient was 21.25 ng/dl after the operation, and the postoperative course was uneventful.

## Discussion

OSCTs are ovarian tumours composed entirely or mostly of cells that secrete steroid hormones. OSCTs can secrete one or more steroid hormones, such as androgens, oestrogen, cortisol, aldosterone, and progesterone, resulting in corresponding symptoms and signs, such as hyperandrogenaemia, hyperestrogenaemia, Cushing syndrome, and refractory hypertension [7], and androgenaemia is the most common. In female hyperandrogenism, adrenal and/or ovarian sources need to be distinguished. The cause of hyperandrogenaemia caused by adrenal tumours is the secretion of excessive dehydroepiandrosterone sulphate [8], and the androgens secreted by most ovarian tumours are not regulated by gonadotropins or adrenocorticotrophic hormone (ACTH). Therefore, adrenal CT and medium-dose dexamethasone suppression tests can be used to exclude adrenal sources.

The clinical manifestations of OSCTs are determined by the steroid hormones produced, and OSCTs can be divided into high-androgen types and high-oestrogen types. Most OSCTs (80%) are of the high-androgen type, and approximately 20% of OSCTs are of the high-oestrogen type [9, 10]. High-androgen-type tumours mainly cause symptoms such as hirsutism, acne, a low and thick voice, an enlarged clitoris, laryngeal knots, breast atrophy, hair loss, and a low posterior hairline. High-oestrogen-type tumours mainly cause symptoms such as irregular vaginal bleeding and endometrial hyperplasia. All patients in this case series exhibited high-androgen-type OSCTs. In case 1, the patient showed progressive hirsutism, and the patients in cases 2 and 3 showed no obvious clinical symptoms. Some scholars [3] conducted a pathological review of approximately 90 OSCT cases reported in domestic and foreign literature from 2000 to 2017 and found that the corresponding clinical manifestations caused by endocrine abnormalities were the main clinical features of OSCTs, but there were still approximately 6% of patients with clinical manifestations with no obvious correlation with endocrine abnormalities.

Due to the low incidence of OSCTs, corresponding imaging reports are rare, and most of them are case reports, so the typical imaging features are not fully understood. On histology, OSCTs are generally well-defined and spherical, while LCTs are significantly smaller than SCT-NOS lesions. OSCTs are dominated by solid components; because most of them contain fat components, they were once called lipocytomas. On microscopy, the tumour cells are rich in lipids, and there are abundant capillary networks and vascular sinusoid structures in the tumour<sup>[11]</sup>. Ultrasound is the first choice for the detection and diagnosis of ovarian tumours due to its convenience, speed and non-invasiveness. OSCTs tend to occur in one ovary, and grey-scale ultrasound usually shows solid, round or oval nodules with clear boundaries. The internal echo is mainly slightly hyperechoic. The echo intensity may be related to the internal fat content. Because testosterone has the effect of increasing vasodilatory substances, most OSCTs exhibit rich blood flow signals dominated by low-resistance blood flow<sup>[12]</sup>. Tan et al.<sup>[13]</sup> performed contrast-enhanced ultrasound in two cases of OLCs and found that the LCTs had a rich blood supply, and the new capillaries around the tumours were more obvious than those in the tumours. Since LCTs are very small and lack typical imaging features, this may cause poor visibility on ultrasound and CT examinations<sup>[14, 15]</sup>. At the same time, in menopausal women, due to the reduced oestrogen level and insufficient perfusion by the ovarian artery blood, the appearance of the ovaries is reduced, and the echo of the ovaries is increased. CDFI usually indicates no blood flow signals in the ovaries<sup>[16]</sup>. Therefore, it is difficult to distinguish between OLC tissue and normal atrophic ovarian tissue by ultrasound. At present, it is believed that SCT-NOS lesions are more easily recognized on imaging than LCTs.

Mature teratomas contain liquid fat and appear as a clear hyperechoic mass on grey-scale ultrasound. Thus, teratomas need to be differentiated from OSCTs. Especially when a small, hyperechoic mass appears on one ovary in menopausal women, the possibility of an OLC cannot be ignored. However, most teratomas are mixed tumours with cystic and solid component. Lipid stratification can occur in the cystic part, and some of the lesions can contain bone tissue or teeth, appearing as hyperechoic nodules with rear acoustic shadows. CDFI usually shows no obvious blood flow signal these masses. Because teratomas contain very few non-secretory tissues that produce testosterone, they very rarely cause hyperandrogenism<sup>[17]</sup>.

Follicular membrane cell tumours that secrete oestrogen are composed of lipid-rich ovarian membrane cells. Histologically, these tumours are mainly solid, with a hard texture and intact capsule, which can be combined with various forms of degeneration, such as calcification. On grey-scale ultrasound, these tumours appear as a round or lobulated, hypoechoic mass with a smooth surface and are often accompanied by varying degrees of posterior sound attenuation, with clear or unclear boundaries; the internal echoes may be uniform or uneven. CDFI shows no obvious blood flow signals in these tumours, and oestrogen secretion is the main distinguishing feature of OSCTs<sup>[18]</sup>. McGonagall syndrome can occur when the tumour is large.

Follicular membrane fibroids are derived from spindle-shaped collagen fibroblasts. They are sex cord-stromal tumours that occur in perimenopausal or postmenopausal women, with very few malignant

changes. Follicular membrane fibromas and follicular cell tumours have similar features on grey-scale ultrasound. CDFI shows that these mass have no blood supply or secretory function, which are key to distinguishing follicular membrane fibromas from OSCTs.

Ovarian Sertoli-Leydig cell tumours, which also commonly show androgen secretion, are composed of Sertoli cells and/or mesenchymal cells of different levels. Histologically, these tumours mainly manifest as a hard, lobulated mass with a complete capsule<sup>[19]</sup>. Unlike OSCT patients, approximately 75% of patients with Sertoli-Leydig cell tumours are 30 years old or younger, and on grey-scale ultrasound, these tumours are mainly solid/cystic masses with clear boundaries. Because the tumour cells contain more fibrous interstitium, the solid part of the tumour is less echogenic. Most of these tumours are rich in blood vessels, so they can show an abundant blood supply on imaging.

Granulosa cell tumours of the ovary are rare, low-grade ovarian stromal tumours with a granular cell morphology, and most secrete oestrogen. Because granulosa cell tumour tissue is fragile and easily becomes detached, causing haemorrhagic necrosis and cystic transformation, solid/cystic masses are typical imaging features of ovarian granulosa cell tumours, and they are mostly arranged in intervals in a radial pattern. CDFI shows minimal to moderate blood flow signals in these tumours<sup>[20]</sup>, with mostly low-resistance blood flow due to the vasodilator effect of oestrogen. It is not difficult to distinguish ovarian granulosa cell tumours from OSCTs using both clinical and imaging features.

When broad ligament leiomyomas become large and show degenerative changes, it is difficult to distinguish them from ovarian tumours. Therefore, accurate positioning of the ovary is the key to distinguishing between the two. Whirlpool or woven hypoechoic masses and pseudocapsules are characteristic ultrasound manifestations of leiomyomas. CDFI shows low blood flow signals inside and around these tumours. Similarly, the lack of endocrine function is also key to distinguishing leiomyomas from OSCTs.

SCT-NOS lesions are the most prone to malignant transformation among OSCTs, with a malignant transformation rate of approximately 25–43%<sup>[12]</sup>. When OSCTs undergo malignant transformation, necrosis, haemorrhage and cystic transformation may occur, and these OSCTs need to be differentiated from ovarian cystadenocarcinomas. Cystadenocarcinomas are malignant ovarian epithelial tumours, with an age at onset later than that of OSCTs. The grey-scale ultrasound features of serous cystic carcinomas include a single sac or cystic mass with compartments, usually accompanied by papillary protrusions. Mucinous cystadenocarcinomas are very large and are usually multilocular cystic masses with solid wall nodules, turbid cyst fluid and poor sound transmission. Since ovarian malignant tumour cells can produce vascular endothelial growth factor, etc., they can induce the formation of new blood vessels lacking smooth muscle tissue, which will lead to a low blood flow RI<sup>[21]</sup>. On CDFI, the solid component of ovarian cystadenocarcinomas shows abundant low-resistance blood flow signals. At the same time, the presence of endocrine function can also help further distinguish the type of tumour.

In summary, the diagnosis of postmenopausal OSCTs is mainly based on typical symptoms and signs, sex hormone determination, imaging features and pathological findings. The corresponding symptoms caused by endocrine abnormalities are the most intuitive clinical manifestations of the disease, especially virilization caused by hyperandrogenaemia, which is more common, but there are still some patients who are completely asymptomatic. A solid, slightly hypoechoic, round or oval mass with a uniform internal echo and an abundant blood supply with low resistance are more typical imaging features of OSCTs. Diagnosing OSCTs is challenging, and surgery can be used for both diagnosis and clear treatment. Of course, histological examination is the gold standard for the final diagnosis of OSCTs.

## **Abbreviations**

OSCT: Ovarian steroid cell tumour; OSCT-NOS: Ovarian steroid cell tumour, not otherwise specified; OLCCT: Ovarian Leydig cell tumour; MRI: magnetic resonance imaging; CT: computed tomography; TVS: transvaginal ultrasound.

## **Declarations**

### **Ethics approval and consent to participate**

Not applicable.

### **Consent to publish**

Written informed consent for publication of images in the article and any accompanying images was obtained from patients.

### **Availability of data and materials**

All the data supporting our findings are contained within the manuscript.

### **Competing interests**

The authors declare that they have no competing interests.

### **Funding**

The authors declare that they have no funding support.

### **Authors' contributions**

XDZ drafted the manuscript, collected the data, and reviewed the literature. LYZ and JJ performed the histological examination and reviewed the manuscript. TAJ provided academic help. NO critically reviewed the manuscript. All authors have confirmed and approved the final manuscript.

## Acknowledgements

The authors thank Dr LinYu Zhou and Dr Jian Jiang for helpful advice and Professor TianAn Jiang of the Ultrasound Medicine Department for discussion and manuscript revision.

## References

1. Alpanes M, Gonzalez-Casbas JM, Sanchez. J, et al. Management of postmenopausal virilization [J]. *J Clin Endocrinol Metab*, 2012, 97(8): 2584–2588.
2. Souto SB, Baptista PV, Braga DC, et al. Ovarian Leydig cell tumor in a post-menopausal patient with severe hyperandrogenism. *Arq Bras Endocrinol Metab*. 2014;58:68–70.
3. Wang Jing Wu, Huanwen L, Zhiyong. Clinical analysis of 19 cases of ovarian steroid cell tumor [J]. *J Diagnostic Pathol*, 2017, 8(24): 561–569.
4. Freitas ACL, Lima J. Leydig cell tumour of the ovary-a case report. *Revista da Faculdade de Ciências Médicas dSorocaba*. 2014;16:152–4.
5. Amneus MW, Natarajan S. Pathologic quiz case: a rare tumor of the ovary [J]. *Arch Pathol Lab Med*, 2003, 127(7): 890–892.
6. Smith D, Crotty TB, Murphy JF, et al. A steroid cell tumor outside the ovary is a rare cause of virilization [J]. *Fertil Steril*. 2006;85(1):227.
7. Dinc G, Saygin I, Kart C, et al. A rare case of postmenopausal severe virilization: ovarian steroid cell tumour, not otherwise specified [J]. *Cases Obstet Gynecol*. 2016;3(1):19–21.
8. Burger HG. Androgen production in Women. [J] *Fertil Steril*. 2002;77(4):3–5.
9. Vulink AJ, Vermes I, Kuijper P, et al. Steroid cell tumour not otherwise specified during pregnancy: a case report and diagnostic work-up for virilisation in a pregnant patient [J]. *Eur J Obstet Gynecol Reprod Biol*. 2004;112(2):221–7.
10. Hayes M, Scully R, et al. Ovarian steroid cell tumors (not otherwise specified). A clinicopathological analysis of 63 cases [J]. *Am J Surg Pathol*, 1987, 11(11): 835–845.
11. Murhekar K, Louis R, Majhi U. A rare occurrence of a steroid cell tumor of the pelvic mesentery: a case report [J]. *J Med Case Rep*, 2011, 5: 517.
12. Lee J, John VS, Liang SX, et al. Metastatic malignant ovarian steroid cell tumor: A case report and review of the literature [J]. *Case Rep Obstet Gynecol*, 2016, 2016: 6184573.
13. Tan BiJun, Chen LinXia. Two cases of ovarian Leydig cell tumor with contrast-enhanced ultrasound. *Chinese Journal of Ultrasound in Medicine*. 2020, 36(5).
14. Shanbhogue AKP, Shanbhogue DKP, Prasad SR, et al. Clinical syndromes associated with ovarian neoplasms: a comprehensive review. *Radiographics*. 2010;30:903–19.
15. Palha Ana, Luísa Cortez AP, Tavares A, Agapito. Leydig cell tumour and mature ovarian teratoma: rare androgen-secreting ovarian tumours in postmenopausal women. *BMJ Case Rep* 2016.

16. Demidov VN, Lipatenkova J, et al. Imaging of gynecological disease(2): clinical and ultrasound characteristics of Sertoli cell tumors, Sertoli–Leydig cell tumors and Leydig cell tumors. *Ultrasound Obstet Gynecol.* 2008;31:85–91.
17. Hoffman JG, Strickland JL, Yin J. Virilizing ovarian dermoid cyst with leydig cells. *J Pediatr Adolesc Gynecol.* 2009;22:e39–40.
18. Li ShengHua, GengXi S, HaiFeng M. Comparative Analysis of MR Manifestations and Pathology of Ovarian Follicle Cell Tumor. *J Journal of Practical Radiology.* 2016;32(1):156–9.
19. Schultz KAP, Harris AK, Schneider DT,et al. Ovarian Sex Cord- Stromal Tumors [J].*JOP*,2016,12 (10) : 940–946.
20. Qin Y,Xue Ensheng ,Liang Rongxi ,et al.The value of color Doppler ultrasound in diagnosis and differential diagnosis of ovarian granulosa cell tumor.*Chin J Ultrasonogr*,December 2017,Vol 26 ,No 12: 1079–1083.
21. Gavalas NG, Lontos M, et al. Angiogenesisrelated pathways in the pathogenesis of ovarian cancer[J]. *Int JMol Sci*,2013,14(8):15885– 15909.

## Figures



**Figure 1**

A: A slightly hyperechoic nodule with an unclear boundary in the right ovary(Case1). B: The left ovary showed a slightly hyperechoic mass with clear borders(Case2). C: A solid, slightly hyperechoic mass with clear boundaries in the left ovary (Case3).

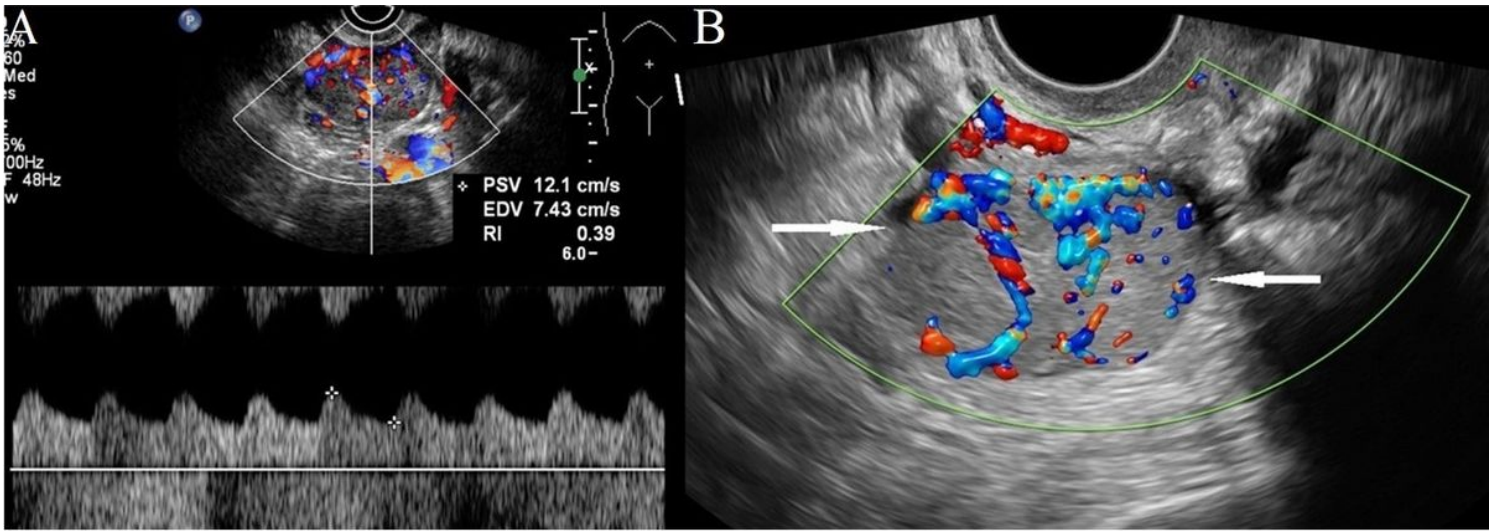


**Figure 2**

A: CDFI showed an abundant blood supply with a resistance index of 0.39(Case 2). B: CDFI showed an abundant blood supply in the mass(Case 3).

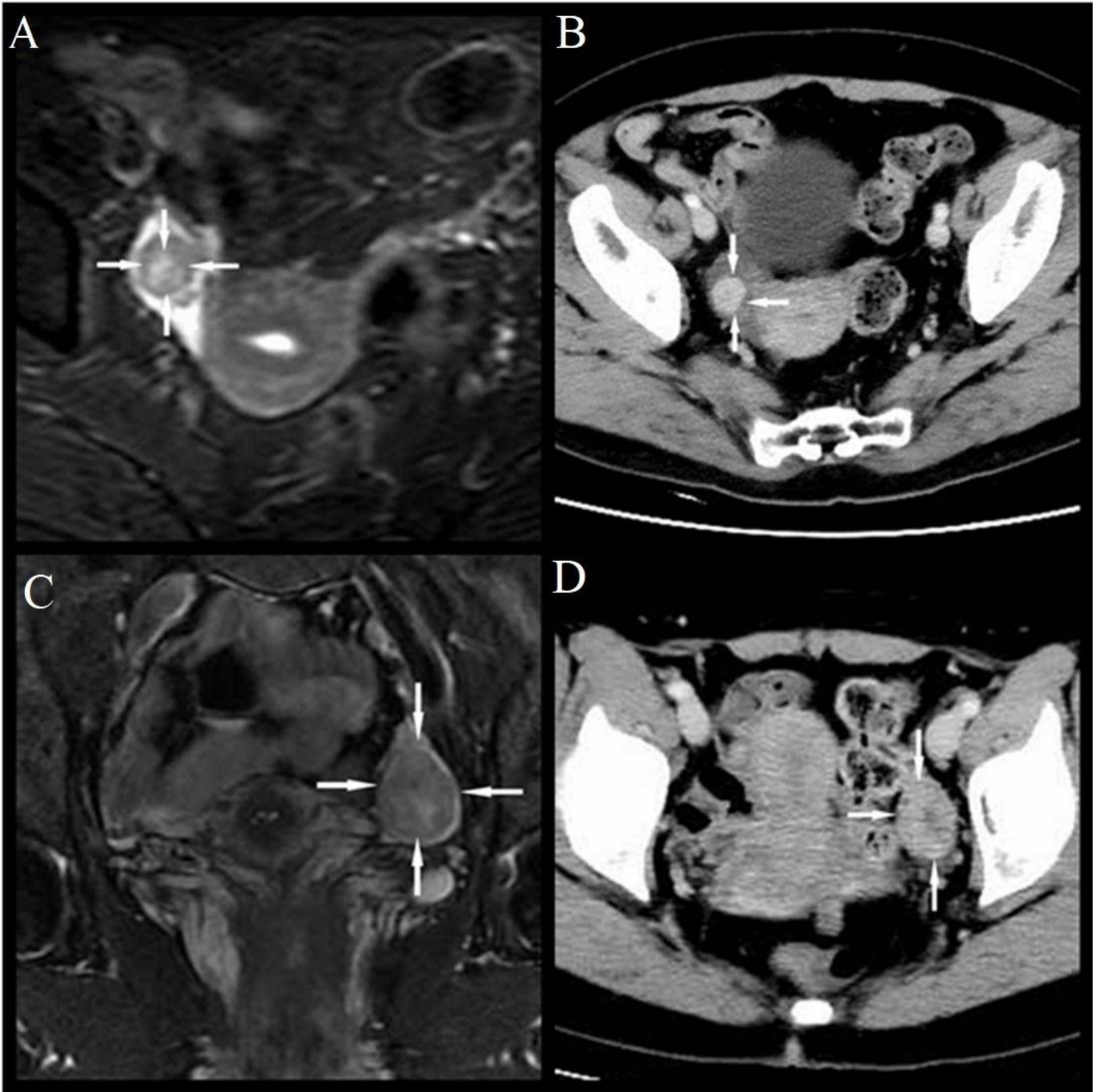


**Figure 3**

A: Enhanced MRI of the pelvis showed nodule in the right adnexal area (Case1). B: Contrast CT of the pelvis showed high-density shadows in the nodular tip of the right adnexal area (Case1). C: Enhanced MRI of the pelvis revealed a space-occupying mass in the left adnexal area(Case 2). D: Enhanced CT of the pelvis showed a solid/cystic mass in the left adnexal area(Case 3).

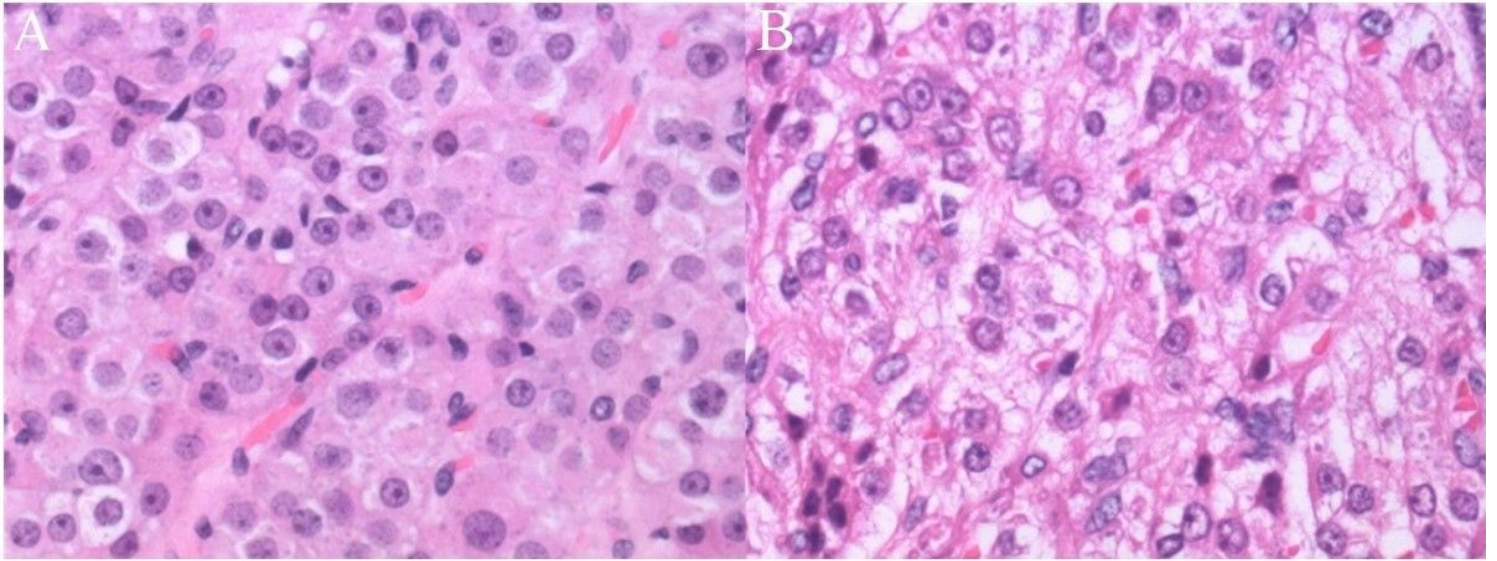


**Figure 4**

A:Haematoxylin-eosin staining by microscopy, magnification 400×(C) showed Leydig cell tumours(Case1). B:Haematoxylin-eosin staining by microscopy, magnification 400×(C) showed Steroid cell tumour, not otherwise specified (Case 2 and Case 3).